

Droplet-based *in situ* compartmentalization of chemically separated components after isoelectric focusing in a Slipchip†

Cite this: *Lab Chip*, 2014, 14, 555

Yan Zhao,^a Fiona Pereira,^b Andrew J. deMello,^b Hywel Morgan^{*a} and Xize Niu^{*c}

Isoelectric focusing (IEF) is a powerful and widely used technique for protein separation and purification. There are many embodiments of microscale IEF that use capillary or microfluidic chips for the analysis of small sample volumes. Nevertheless, collecting the separated sample volumes without causing remixing remains a challenge. Herein, we describe a microfluidic Slipchip device that is able to efficiently compartmentalize focused analyte bands *in situ* into microdroplets. The device contains a microfluidic “zig-zag” separation channel that is composed of a sequence of wells formed in the two halves of the Slipchip. The analytes are focused in the channel and then compartmentalised into droplets by slipping the chip. Importantly, sample droplets can be analysed on chip or collected for subsequent analysis using electrophoresis or mass spectrometry for example. To demonstrate this approach, we perform IEF separation using standard markers and protein samples, with on-chip post-processing. Compared to alternative approaches for sample collection, the method avoids remixing, is scalable and is easily hyphenated with the other analytical methods.

Received 19th September 2013,
Accepted 6th November 2013

DOI: 10.1039/c3lc51067k

www.rsc.org/loc

Introduction

Isoelectric focusing (IEF) is a technique that separates and focuses complex mixtures of amphoteric molecules (such as peptides and proteins) according to their isoelectric points (pI)s.¹ IEF is widely and routinely used in proteomics, and is recognised to be one of the most powerful techniques for protein purification and separation.

There are many embodiments of the IEF separation process. For example, immobilized pH gradient (IPG) gel-based IEF is commonly used as the first dimension in two-dimensional gel electrophoresis.^{2–4} IEF in capillaries (cIEF)^{5,6} and chip-based microfluidic devices (μ IEF)^{7,8} has also been developed, using carrier ampholytes (CA) to generate pH gradients.^{9,10} cIEF and μ IEF consume extremely small amounts of sample compared to other methods and have the potential for high throughput operation and automatic

hyphenation to downstream analytical methods such as electrophoresis or mass spectrometry.^{11–13} Miniaturized two-dimensional electrophoresis systems have been presented.¹⁴ However, hyphenation of miniaturised IEF platforms with other analytical methods is not without challenges. Indeed, a significant hurdle remains in how to collect the discrete separated bands for subsequent transfer to a downstream analytical system. The focused analyte can be removed from the capillary or microchannel by pressure-driven flow,^{13,15,16} electroosmotic flow or chemical mobilization.^{17,18} However, these methods introduce dispersion and remixing of the focused bands during sample migration, negating many advantages of the technique. To address this limitation, a method to cut the separated sample into 8 fractions was presented;¹⁹ similarly, there are papers describing IEF separation in a droplet followed by splitting into two halves after separation.^{20,21} These methods do not need to mobilize the sample for fractionation, avoiding the remixing in the migration, but the resolution is very low. Free flow IEF is a new embodiment of microfluidic based separation, where IEF is performed in a laminar flow. The separated species are collected by dividing the flow stream into several different outlets,^{22,23} and a system that can compartmentalize the separated sample into 96 fractions has been commercialized (FFE Service GmbH, Munich, Germany). However, free flow IEF consumes samples in mg quantities, much more than cIEF or μ IEF, and the miniaturized system has not yet

^a Faculty of Physical Sciences and Engineering, and Institute for Life Sciences, University of Southampton, Highfield, Southampton, SO17 1BJ, UK.
E-mail: hm@ecs.soton.ac.uk

^b Institute for Chemical and Bioengineering, Department of Chemistry and Applied Biosciences, ETH Zürich, Zürich, Switzerland

^c Faculty of Engineering and the Environment, and Institute for Life Sciences, University of Southampton, Highfield, Southampton, SO17 1BJ, UK.
E-mail: X.Niu@soton.ac.uk

† Electronic supplementary information (ESI) available. See DOI: 10.1039/c3lc51067k

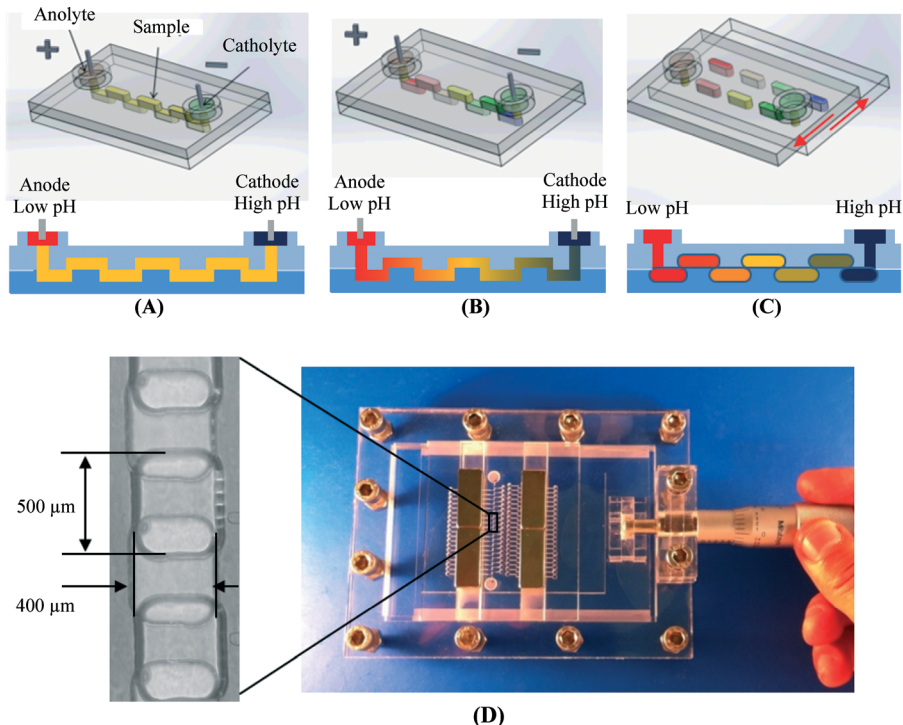


Fig. 1 Schematic drawing of IEF separation and *in situ* compartmentalisation in a Slipchip. (A) Sample loading to a continuous “zig-zag” channel. (B) pH gradient is established and IEF is performed after application of an electric field. (C) *In situ* compartmentalisation after IEF separation. (D) The microdevice and platform made of PMMA, containing a “zig-zag” channel with dimensions of $400\ \mu\text{m} \times 250\ \mu\text{m} \times 5\ \text{cm}$ ($500\ \mu\text{m}$ long for each well).

demonstrated high separation resolution and throughput. Very recently, Wang *et al.* presented a rotary valve which can create fractions after IEF in a capillary loop.²⁴ The analyte collection is diffusion free, but the system is very complicated.

In recent years, microdroplets formed within microfluidic channels have been developed as tools for compartmentalizing chemically separated components. For example, Niu *et al.* demonstrated compartmentalisation of samples separated by both liquid chromatography^{25,26} and capillary gel electrophoresis,²⁷ and Chiu and co-workers presented segmentation of CE separated sample into nL-volume droplets.^{28,29} In each case, the droplets could be further analysed using CE²⁵ or MS.^{26,29} However, it should be noted that compartmentalisation is typically performed at a fixed point (normally at the outlet) for both LC and CE. Such an approach is not applicable to IEF, where focused analytes are distributed along the pH gradient.

In the current paper, we describe a Slipchip-based method that achieves *in situ* compartmentalization of an IEF separated sample into droplets. The separated droplets can be collected and moved with ease for further downstream analysis. The Slipchip is a microfluidic format, introduced by Ismagilov and co-workers, and generates droplets in parallel by slipping (or moving) layers of a planar chip to different lateral positions.^{30,31} Compared to conventional microfluidic systems that incorporate closed channels, a Slipchip is made of two unsealed halves containing open channels. Multiple wells and ducts can be patterned on each half, with the chip having different functions depending on the relative positions of the two halves. Such Slipchips have been used in a

variety of applications including digital polymerase chain reaction,³² screening of protein crystallisation,^{33,34} and multi-step biological assays.³⁵

Herein, we re-engineered the original Slipchip format to incorporate a microfluidic IEF separation followed by *in situ* compartmentalisation as shown schematically in Fig. 1A–C. The working principle is as follows: an IEF separation is first performed in a microfluidic zig-zag channel that is composed of a sequence of wells formed in the two halves of the Slipchip (Fig. 1A). A pH gradient is then established in this channel and analyte focused along the channel by application of an electric field (Fig. 1B). Slipping the chip disconnects these wells, leaving the analyte in isolated compartments or single droplets in each of the wells (Fig. 1C). This method totally eliminates remixing *via* a single slipping operation. Samples can then be collected for downstream analysis with other methods, or be post-processed on chip.

Experimental

Materials and chemicals

Milli-Q deionised water (Millipore, MA, US) was used throughout. 2 mm thick acrylic sheets were obtained from Nitto Jushi Kogyo Ltd. (Tokyo, Japan), Pharmalyte broad-band carrier ampholytes pH 3–10 were obtained from GE Healthcare Life Sciences (Buckinghamshire, UK), cIEF gel polymer solution was obtained from Beckman Coulter (Buckinghamshire, UK), FC-40 oil was obtained from 3M (Berkshire, UK), and universal pH indicator solution, phosphoric acid (85%), L-arginine,

iminodiacetic acid, polyvinyl alcohol (PVA), hydroxypropyl methylcellulose (HPMC), fluorescence *pI* markers and IEF protein markers were obtained from Sigma-Aldrich (Dorset, UK).

Sample preparation

IEF buffer was prepared from 3 M urea cIEF gel, 3% Pharmalyte pH 3–10 broad-band carrier ampholyte, 0.5 mM iminodiacetic acid, 6 mM L-arginine, and 4% (w/v) PVA. Additionally, 26 mM H₃PO₄ and 4 mM NaOH in cIEF gel with 3% (w/v) hydroxypropyl methylcellulose (HPMC) each were prepared as the anolyte and catholyte, respectively. IEF protein markers were obtained as lyophilized powder and reconstituted according to the manufacturer's instructions, *i.e.* 4 mg mL⁻¹ of protein in 200 mM glycine. 3 μL of each protein solution was mixed in 400 μL IEF buffer to yield a final concentration of 29 μg mL⁻¹. Approximately 7 μL of the mixed sample was used for each IEF run, *i.e.* about 200 ng of each protein.

Device fabrication and platform preparation

The device was formed from two separate acrylic plates, with wells, ducts and holes patterned on each half. Two reservoirs for the anolyte and catholyte were placed on the top plate and connected to the separation channel *via* inlet/outlet holes. The dimensions of each droplet well were 400 μm × 500 μm and 250 μm deep, giving a well volume of 50 nL (Fig. 1D). The separation channel consisted of 140 wells in series, with associated inlet and outlet holes. The total length was 5 cm, giving a total sample volume of 7 μL. The acrylic plates were micro-milled using a LPKF Protomat S100 milling machine (LPKF Laser & Electronics Ltd, Berkshire, UK). After cutting, the plates were rinsed with water and then ultrasonicated in isopropyl alcohol for 10 minutes. The plates were further rinsed with fresh isopropyl alcohol, dried with nitrogen gas and dehydrated at 60 °C for 30 minutes. To produce flat surfaces, the plates were exposed to chloroform vapour for 3 minutes to reflow the surface.³⁶

A hydrophobic coating was deposited on the chip surfaces to prevent leakage and cross-contamination.³⁴ This was achieved by coating the acrylic surface with a 0.5 μm thick parylene C layer, followed by a treatment with Duxcoat Nano solution (Duxback Ltd, Somerset, UK), and finally drying in an oven at 60 °C for 10 minutes. The devices were held in a specially designed chip holder with two pairs of magnets being used to clamp the plates together. A micrometer head was used to precisely control the slipping distance. Fig. 1D shows an image of the entire device.

Device preparation

300 μm diameter platinum wires were used as electrodes and connected to an LKB 2197 high voltage DC power supply (LKB, Bromma, Sweden). The electric current was monitored continuously and the device was imaged with a Zeiss LSM 5 confocal fluorescence microscope using a DAPI filter set.

Prior to use, FC-40 oil was applied between the two plates to wet both surfaces. The oil creates a seal preventing

leakage³⁰ and also acts as a lubricant. Two pairs of magnets were used to clamp the plates with an average clamping force at about 0.2 kg cm⁻². The clamping force was found to be strong enough to prevent leakage but also allows the chips to be slipped. After chip assembly, excess oil was removed by flowing air through the device, with any remaining oil in the reservoirs being removed with a pipette. The 7 μL IEF sample buffer was injected into the separation channel at a flow rate below 100 μL min⁻¹, and no leakage was observed. Reservoirs were loaded with electrolyte, and the electrodes were connected to the high voltage power supply to give an electric field of 100 V cm⁻¹.

Results and discussions

IEF separation

Initially, the wells on both plates were aligned and connected to form a continuous “zig-zag” channel. Then the samples (fluorescence *pI* markers: *pI* 4.0, 6.2, and 8.1, Sigma-Aldrich, UK) were mixed with carrier ampholyte and loaded into the channel. 3% (w/v) HPMC was also added to the mixture to reduce electro-endosmosis and increase the viscosity of the medium (see the ESI†). Subsequently, anolyte and catholyte were separately loaded into the reservoirs, followed by platinum electrodes (Fig. 1A). IEF was performed using an electric field strength of 100 V cm⁻¹ for 30 minutes. Focusing of the *pI* markers was monitored with the confocal microscope. The entire channel was imaged by moving the chip with respect to the microscope objective. One scan was performed every minute for the first 5 minutes, and then once every 5 minutes thereafter (Fig. S6†). At the beginning of an experiment, the current was at its peak value of 180 μA (Fig. S7†), and the fluorescent *pI* markers were uniformly distributed in the channel, producing a uniform fluorescence intensity. After 30 minutes of focusing, the three fluorescence markers were at their *pI*s, with three fluorescence peaks clearly visible. At this point, the current had dropped to a stable value about 12 μA. The focusing time varies in different IEF systems with different capillary/channel dimensions, electrical field strength, chemical protocol, *etc.*, compared to other published IEF platforms;^{5–13} the 30 minutes focusing time in our system is reasonable.

Anodic and cathodic drifts affect the stability and reproducibility in cIEF. Here we used L-arginine (Arg) and iminodiacetic acid (IDA) as anodic and cathodic stabilizers to eliminate the drifts. Mack *et al.*³⁷ optimised the protocol and used H₃PO₄ and NaOH as anolyte and catholyte solutions, and Arg and IDA as barriers between IEF buffer and electrolyte, which is a standard protocol now for commercialized cIEF system (Beckman Coulter, Inc.). Fig. 2 shows the average distance of the focused *pI* markers from the anodic end of the device, obtained from 25 repeats on 5 different devices. It can be seen that the position of the *pI* 4.0 marker is highly reproducible with a relative standard deviation (RSD) of less than 3%. However, the error bar is larger for the *pI* 6.2 marker, with RSD about 4%, and worse for the *pI* 8.1 marker,

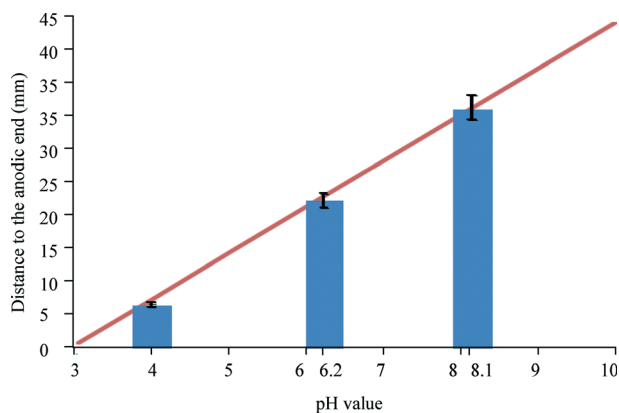


Fig. 2 Average distance of the focused *pI* markers (*pI* 4.0, 6.2 and 8.1) from the anodic end of the device. Data were collected from 5 similar devices for 25 repeats, after 30 minutes of focusing at an applied field of 100 V cm^{-1} . The error bars indicate the standard deviations.

with RSD about 7%. This was also observed by Mack *et al.*³⁷ and attributed to isotachopheresis (ITP). The time trace fluorescence intensity curve shown in Fig. S6† also suggests that after about 25 to 30 minutes, ITP tends to dominate over IEF in the channel. This problem has been studied for decades,^{10,37–40} but further effort is still needed to optimise the protocol. IEF separations were also performed using the same chip and buffers, but without the FC-40 oil between the plates, yielding similar peak positions. Nevertheless, the average RSD of 4.9% from Fig. 2 confirms that IEF separations can be performed reproducibly in the Slipchip. Moreover, the positions of the three known *pI* markers fit with a linear distribution of pH gradient in the channel.

In situ compartmentalisation

In situ compartmentalisation can be readily achieved by slipping the chip to disconnect the zig-zag channel. We used a food dye to show droplet generation as illustrated in Fig. 3. Two rows of droplets (140 in total) were formed in wells, without any discernible leakage. IEF separation was performed in the same chip using six *pI* markers (*pI* 4.0, 5.5, 7.2, 7.6, 8.1 and 9.0) as shown in Fig. 4A. The peak capacity of IEF separation can be calculated as $n = L/w \approx 140$, where L is the total channel length and w is a measure of the average analyte half peak bandwidth. Accordingly, the theoretical minimum resolvable difference in isoelectric point $\Delta(pI)$ is equal to 0.05. Such separation results are comparable with previously reported μ IEF systems^{7,8,41,42} where peak capacities range from 36 to 133.

After 30 minutes of IEF, the device was slipped perpendicular to the direction of the separation channel and the

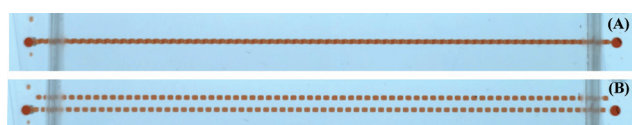


Fig. 3 Bright field microscopy image of the zig-zag channel filled with red dye. (A) Before slipping and (B) after slipping, and 140 droplets were generated.

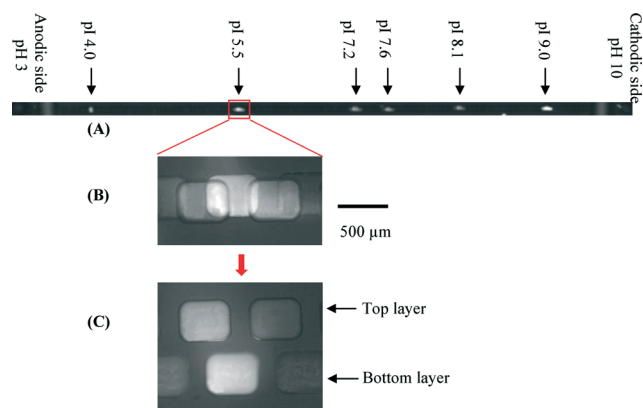


Fig. 4 Fluorescence image of six focused *pI* markers (*pI* 4.0, 5.5, 7.2, 7.6, 8.1 and 9.0) in a zig-zag channel. (A) The whole channel before compartmentalization; (B) The focused *pI* 5.5 marker before compartmentalization; (C) by slipping the chip, the focused *pI* 5.5 marker was compartmentalized into a droplet in a well.

focused *pI* markers were encapsulated into droplets, as shown in Fig. 4B and C for a selected area. The electric field was maintained during slipping until the wells were completely separated and discrete droplets were created. The compartmentalisation time depends on the relative movement of the blocks; however, the process typically takes less than one second. In addition, the Reynolds number was calculated to be 0.0001, confirming that the flow is laminar during chip slipping and no turbulence is induced; therefore, no remixing occurs along the lateral direction of the channel. It should be noted that after compartmentalisation, the analytes located in the same well (droplet) are mixed by molecular diffusion; therefore, it is crucial that the number of wells in each chip should be at least equal to the peak capacity of the separation, to prevent remixing of two or more focused peaks.

During slipping, no fluorescence was detected outside the wells, meaning that the oil prevents sample leakage and loss of sample. However, the Duxcoat hydrophobic coating can degrade with time, causing some leakage between the plates. Therefore, the substrates were re-coated with Duxcoat after three experiments. The parylene coating lasts much longer, but after approximately 50 runs, the PMMA chip was disposed of.

Droplet collection

Two methods were developed for collecting the compartmentalized droplets for further analysis, namely parallel collection and serial collection. The process of serial collection is shown in Fig. 5A and B; two zig-zag collection channels were placed on each side of the main separation channel and pre-filled with oil; the outlets of the collection channels were connected to tubing to collect the droplets. After compartmentalization, discrete droplets were further moved to meet with the collection channels, forming a continuous conduit. The separated droplets could be collected into tubing for further analysis. We have recently demonstrated spotting

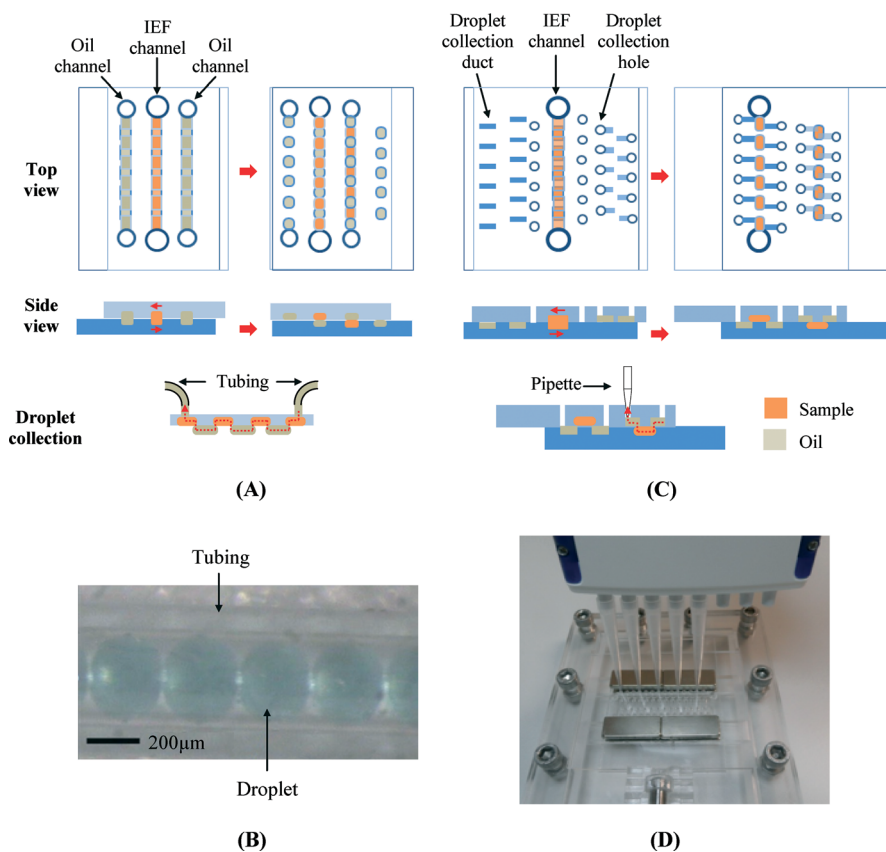


Fig. 5 Serial and parallel droplet collection. (A) Schematic of serial droplet collection. Two zig-zag collection channels are placed on each side of the main separation channel and pre-filled with oil. The outlets of the collection channels are connected to tubing to collect droplets. (B) Microscope image of serially collected droplets in a length of tube. (C) Schematic of parallel droplet collection. Collection ducts and holes are fabricated on each side of the separation channel. After compartmentalization, the droplets are moved to the interface with the collection ducts and holes facilitating droplet collection in parallel using a multichannel pipette. (D) Photograph of parallel droplet collection with a pipette.

of droplets onto a target plate for matrix-assisted laser desorption/ionization MS²⁶ and injecting the whole droplet into a separation channel to achieve droplet interfaced microchip and capillary electrophoretic separations.⁴³

The parallel collection is shown schematically in Fig. 5C. Collection ducts and holes were fabricated on each side of the separation channel. After compartmentalization, the droplets were further moved to meet the collection ducts and holes. Droplets were collected in a single step using a multichannel pipette (Fig. 5D). This parallel collection method is especially suitable for on-demand collection of droplets, for example, when collecting only those droplets containing analytes at certain *pI* values of interest. For this method, due to the extra collection ducts and holes that need to be introduced, the well density cannot be as high as the serial collection channel design because of fabrication limits. A device with 29 wells is demonstrated here, the dimension of each well is 250 μm \times 1.7 mm, each droplet covers a *pH* range of 0.24 and the collection efficiency was measured at 91(\pm 6)% for 7 separate operations.

Protein separation

As a proof of principle for the entire system, we performed an IEF separation of a mixture containing 5 standard

proteins, trypsin inhibitor, β -lactoglobulin A, carbonic anhydrase isozyme II, myoglobin, and lectin. After 30 minutes with the same conditions used previously, the sample was compartmentalised into droplets and the droplets were collected using the parallel collection method and subsequently analysed by microchip electrophoresis using an Agilent 2100 Bioanalyzer.

A total of 21 single droplets were collected using the parallel collection device, covering the *pH* range from 3.7 to 8.6. To simplify verification, these droplets were further mixed with 3 consecutive droplets, and diluted to give a total sample volume of 4 μL . These sample droplets were analysed directly using the Bioanalyzer to obtain electropherograms as shown in Fig. 6. Lane 8 defines the control (mixtures containing all 5 proteins) with all 5 bands. The other gel lanes show the results obtained from each combined sample droplet. Lane 1 covers the *pH* range from 3.7 to 4.4. There is no protein in this range. Lane 2 covers the *pH* range from 4.4 to 5.1, where the trypsin inhibitor can be found. β -Lactoglobulin A has a *pI* of 5.1 and appears in lane 3. Carbonic anhydrase isozyme II, trypsin inhibitor and myoglobin appear in lanes 4, 6 and 7, respectively. The carrier ampholyte and urea can often affect resolution in CE. Although all of the bands can be distinguished in the

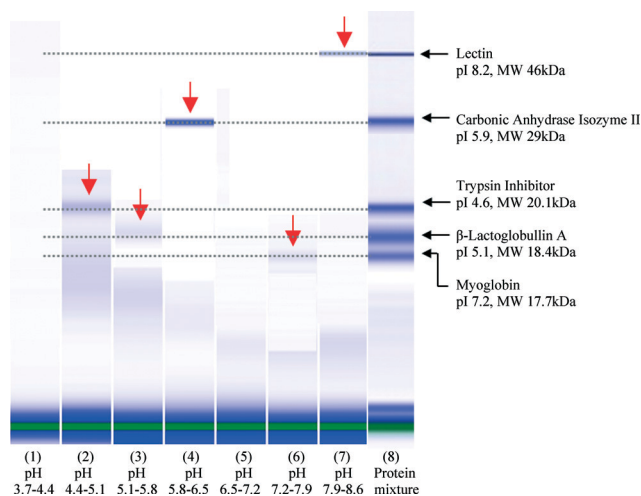


Fig. 6 Gel electropherogram of collected droplets, processed with an Agilent 2100 Bioanalyzer. The sample contains five proteins with different pI/s and molecular weights, as indicated on the right.

electropherogram in Fig. 6, the bands in lanes 2, 3 and 6 are smeared. Additionally, the intensities of these bands are weaker than that in the control lane due to sample dilution. Desalting samples, using chloroform-methanol protein extraction,⁴⁴ could reduce the effects of Joule heating and stabilize current during the electrophoresis, but the process is time consuming and requires delicate fluidic operations of small samples. Another possible method of increasing resolution is to analyse the samples with ‘native electrophoresis’ as shown by Emrich *et al.*,¹⁴ where 7 M urea was actually included into the electrophoresis matrix to increase reproducibility of the separation.

On-chip post-processing and pH gradient indication

The system is also capable of on-chip post-processing; the separated droplets can be mixed and reacted with other on-chip generated reagent droplets. To demonstrate this, a continuous pH gradient was created in the Slipchip. Accurate pH gradient formation is a critical step in an IEF process. Ideally, the pH distribution should be known throughout the entire channel, so that a focused unknown protein can be reliably allocated to a pH point or range, or known proteins collected according to their pI/s. However, whole channel/capillary pH gradient calibration is difficult to achieve in μ IEF or cIEF. Previously, pH gradient calibration has been performed either by measuring the position of pI markers⁴⁵ or by premixing a pH indicator into the sample.^{20,21} In the former method, the pH values need to be interpolated where markers are unavailable; in the latter, the pH indicator may influence sample and buffer conditions.

Here we demonstrate an on-chip indication method. Channels for the pH indicator solution were fabricated on each side of the IEF separation channel. After IEF separation, the top layer plate was slipped, and both the sample and the pH indicator were compartmentalized into droplets in the wells. Following additional plate manipulation, the sample

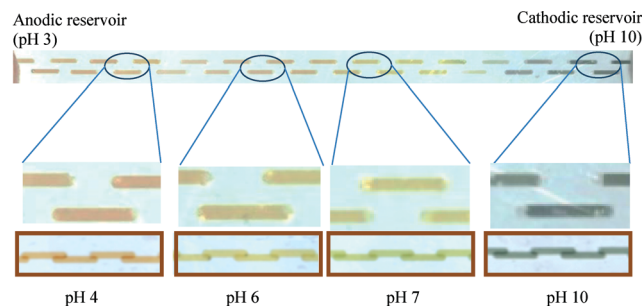


Fig. 7 Colour image showing on-chip pH gradient calibration. Bottom panels show controls for each representative pH value.

and pH indicator droplets in different layers were merged and mixed. After 10 minutes, the plate was moved back, and an image of the entire channel was obtained as shown in Fig. 7. The colour distribution in the channel was compared with images from the other channels containing mixtures of pH indicator with known pH values (standard pH buffer of pH 4, 6, 7 and 10), as shown in the inset of Fig. 7 for representative pH values. It was found that all the images show colorimetric similarity to their corresponding pH points, suggesting that a continuous and near linear pH gradient can be reliably established in Slipchip-based IEF channels. It should also be noted that the current method of visual comparison is somewhat limited, and the resolution of the broadband pH indicator solution is not high. Further efforts are required to calibrate an accurate pH gradient.

Conclusions

We have demonstrated a novel, chip-based IEF system that can perform high resolution *in situ* compartmentalization of a separated sample into droplets. The fractionation process does not need to mobilise the focused species, eliminating the re-mixing problem that occurs in other methods. The functionality of the device was demonstrated using standard IEF markers. Droplets can be collected either in parallel or serial and transferred for further analysis off-chip. Five standard proteins were separated and analysed downstream with chip-based gel electrophoresis. The reported device is also capable of on-chip post-processing; pH gradient on-chip indication has been demonstrated. The reported device has the potential to dramatically reduce the volume of each partition, to analyse complex proteomic samples, and to be hyphenated with the other analytical devices for multidimensional separations.

Acknowledgements

Niu and Morgan would like to thank EPSRC ‘Bridging The Gap’ for funding the research. We also thank Yu Zhang for fabricating some of the microdevices. de Mello would like to acknowledge partial support from ETH Zürich and the Global Research Laboratory Program of the National Research Foundation of Korea (grant number K2090400004-11A0500-00410).

References

- 1 A. Kolin, *Proc. Natl. Acad. Sci. U. S. A.*, 1955, **41**, 101–110.
- 2 A. Gorg, G. Boguth, C. Obermaier and W. Weiss, *Electrophoresis*, 1998, **19**, 1516–1519.
- 3 M. Pernemalm and J. Lehtio, *J. Proteome Res.*, 2013, **12**, 1014–1019.
- 4 E. Gianazza and P. G. Righetti, *Electrophoresis*, 2009, **30**, S112–S121.
- 5 L. H. H. Silvertand, J. S. Torano, W. P. van Bennekom and G. J. de Jong, *J. Chromatogr., A*, 2008, **1204**, 157–170.
- 6 P. G. Righetti, R. Sebastiano and A. Citterio, *Proteomics*, 2013, **13**, 325–340.
- 7 J. J. Ou, T. Glawdel, C. L. Ren and J. Pawliszyn, *Lab Chip*, 2009, **9**, 1926–1932.
- 8 H. C. Cui, K. Horiuchi, P. Dutta and C. F. Ivory, *Anal. Chem.*, 2005, **77**, 1303–1309.
- 9 G. J. Sommer and A. V. Hatch, *Electrophoresis*, 2009, **30**, 742–757.
- 10 P. G. Righetti, A. Citterio and H. Girault, *Electrophoresis*, 2007, **28**, 1860–1866.
- 11 L. H. H. Silvertand, J. S. Torano, G. J. de Jong and W. P. van Bennekom, *Electrophoresis*, 2009, **30**, 1828–1835.
- 12 N. G. Weiss, N. L. Zwick and M. A. Hayes, *J. Chromatogr., A*, 2010, **1217**, 179–182.
- 13 W. J. Yu, Y. Li, C. H. Deng and X. M. Zhang, *Electrophoresis*, 2006, **27**, 2100–2110.
- 14 A. Emrich, I. L. Medintz, W. K. Chu and R. A. Mathies, *Anal. Chem.*, 2007, **79**, 7360–7366.
- 15 T. L. Huang, P. C. H. Shieh and N. Cooke, *Chromatographia*, 1994, **39**, 543–548.
- 16 Y. M. Hua, B. M. Koshel and M. J. Wirth, *Anal. Chem.*, 2010, **82**, 8910–8915.
- 17 L. M. Ramsay, J. A. Dickerson and N. J. Dovichi, *Electrophoresis*, 2009, **30**, 297–302.
- 18 X. F. Zhong, E. J. Maxwell, C. Ratnayake, S. Mack and D. D. Y. Chen, *Anal. Chem.*, 2011, **83**, 8748–8755.
- 19 P. G. Righetti, C. Simo, R. Sebastiano and A. Citterio, *Electrophoresis*, 2007, **28**, 3799–3810.
- 20 A. Egatz-Gomez and W. Thormann, *Electrophoresis*, 2011, **32**, 1433–1437.
- 21 N. G. Weiss, M. A. Hayes, A. A. Garcia and R. R. Ansari, *Langmuir*, 2011, **27**, 494–498.
- 22 J. A. Wen, J. W. Albrecht and K. F. Jensen, *Electrophoresis*, 2010, **31**, 1606–1614.
- 23 J. Wen, E. W. Wilker, M. B. Yaffe and K. F. Jensen, *Anal. Chem.*, 2010, **82**, 1253–1260.
- 24 W. Wang, J. J. Lu, C. Y. Gu, L. Zhou and S. R. Liu, *Anal. Chem.*, 2013, **85**, 6603–6607.
- 25 X. Z. Niu, B. Zhang, R. T. Marszalek, O. Ces, J. B. Edel, D. R. Klug and A. J. de Mello, *Chem. Commun.*, 2009, 6159–6161.
- 26 F. Pereira, X. Z. Niu and A. J. de Mello, *PLoS One*, 2013, **8**, e63087.
- 27 M. C. Draper, X. Niu, S. Cho, D. I. James and J. B. Edel, *Anal. Chem.*, 2012, **84**, 5801–5808.
- 28 T. Chiu, *Anal. Bioanal. Chem.*, 2010, **397**, 3179–3183.
- 29 J. S. Edgar, G. Milne, Y. Q. Zhao, C. P. Pabbati, D. S. W. Lim and D. T. Chiu, *Angew. Chem., Int. Ed.*, 2009, **48**, 2719–2722.
- 30 W. B. Du, L. Li, K. P. Nichols and R. F. Ismagilov, *Lab Chip*, 2009, **9**, 2286–2292.
- 31 T. Schneider, J. Kreutz and D. T. Chiu, *Anal. Chem.*, 2013, **85**, 3476–3482.
- 32 F. Shen, W. B. Du, J. E. Kreutz, A. Fok and R. F. Ismagilov, *Lab Chip*, 2010, **10**, 2666–2672.
- 33 L. Li, W. B. Du and R. F. Ismagilov, *J. Am. Chem. Soc.*, 2010, **132**, 106–111.
- 34 L. Li, W. B. Du and R. F. Ismagilov, *J. Am. Chem. Soc.*, 2010, **132**, 112–119.
- 35 W. S. Liu, D. L. Chen, W. B. Du, K. P. Nichols and R. F. Ismagilov, *Anal. Chem.*, 2010, **82**, 3276–3282.
- 36 R. G. Ogilvie, V. J. Sieben, C. F. A. Floquet, R. Zmijan, M. C. Mowlem and H. Morgan, *J. Micromech. Microeng.*, 2010, **20**(6), 065016.
- 37 S. Mack, I. Cruzado-Park, J. Chapman, C. Ratnayake and G. Vigh, *Electrophoresis*, 2009, **30**, 4049–4058.
- 38 Z. Q. Xu, N. Okabe, A. Arai and T. Hirokawa, *Electrophoresis*, 2010, **31**, 3558–3565.
- 39 M. Busnel, T. Le Saux, S. Descroix, H. H. Girault, M. C. Hennion, S. Terabe and G. Peltre, *J. Chromatogr., A*, 2008, **1182**, 226–232.
- 40 C. Pager, A. Vargova, A. Takacs-Nagy, A. Dornyei and F. Kilar, *Electrophoresis*, 2012, **33**, 3269–3275.
- 41 V. Dauriac, S. Descroix, Y. Chen, G. Peltre and H. Senechal, *Electrophoresis*, 2008, **29**, 2945–2952.
- 42 A. J. Hughes, R. K. C. Lin, D. M. Peehl and A. E. Herr, *Proc. Natl. Acad. Sci. U. S. A.*, 2012, **109**, 5972–5977.
- 43 X. Niu, F. Pereira, J. B. Edel and A. J. de Mello, *Anal. Chem.*, 2013, **85**, 8654–8660.
- 44 D. Wessel and U. I. Flugge, *Anal. Biochem.*, 1984, **138**, 141–143.
- 45 K. Shimura, K. Kamiya, H. Matsumoto and K. Kasai, *Anal. Chem.*, 2002, **74**, 1046–1053.